Cellular and Molecular Life Sciences (2020) 77:3013–3026
https://doi.org/10.1007/s00018-019-03338-4

ORIGINAL ARTICLE

Homotrimeric MMP-9 is an active hitchhiker on alpha-2-macroglobulin partially escaping protease inhibition and internalization through LRP-1

Xena Serifova[1] · Estefania Ugarte-Berzal[1] · Ghislain Opdenakker[1] · Jennifer Vandooren[1]

Received: 7 August 2019 / Revised: 27 September 2019 / Accepted: 3 October 2019 / Published online: 23 October 2019

Abstract

Proteolysis is a crucial process in life, tightly controlled by numerous natural protease inhibitors. In human blood, alpha-2-macroglobulin is an emergency protease inhibitor preventing coagulation and damage to endothelia and leukocytes. With the use of a unique protease trapping mechanism, alpha-2-macroglobulin lures active proteases into its snap-trap, shields these from potential substrates and 'flags' their complex for elimination by receptor-mediated endocytosis. Matrix metalloprotease-9/gelatinase B is a secreted protease increased in blood of patients with inflammations, vascular disorders and cancers. Matrix metalloprotease-9 occurs as monomers and stable homotrimers, but the reason for their co-existence remains obscure. We discovered that matrix metalloprotease-9 homotrimers undergo reduced anti-proteolytic regulation by alpha-2-macroglobulin and are able to travel as a proteolytically active hitchhiker on alpha-2-macroglobulin. As a comparison, we revealed that monomeric active matrix metalloprotease-9 is efficiently trapped by human plasma alpha-2-macroglobulin and this masks the detection of activated matrix metalloprotease-9 with standard analysis techniques. In addition, we show that alpha-2-macroglobulin/trimer complexes escape clearance through the receptor low-density lipoprotein receptor-related protein 1, also known as the alpha-2-macroglobulin receptor. Thus, the biochemistry and biology of matrix metalloprotease-9 monomers and trimers are completely different as multimerization enables active matrix metalloprotease-9 to partially avoid alpha-2-macroglobulin regulation both by direct protease inhibition and by removal from the extracellular space by receptor-mediated endocytosis. Finally, for the biomarker field, the analysis of alpha-2-macroglobulin/protease complexes with upgraded technology is advocated as a quotum for protease activation in human plasma samples.

Keywords Proteolysis · α2M · MMP-9 · Endocytosis · LRP-1

Abbreviations

α2M	Alpha-2-macroglobulin
cdMMP-3	Catalytic domain of MMP-3
LRP-1	Low density lipoprotein receptor-related protein-1
MMPs	Matrix metalloproteases
TIMPs	Tissue inhibitors of metalloproteases

Electronic supplementary material The online version of this article (https://doi.org/10.1007/s00018-019-03338-4) contains supplementary material, which is available to authorized users.

✉ Jennifer Vandooren
Jennifer.vandooren@kuleuven.be

[1] Laboratory of Immunobiology, Department of Microbiology and Immunology, Rega Institute for Medical Research, University of Leuven, KU Leuven, Herestraat 49, Bus 1044, 3000 Leuven, Belgium

Introduction

Proteases play important regulatory roles in life, ranging from common physiological processes (e.g. development and growth), to infections (e.g. HIV and parasitic diseases), inflammations (e.g. asthma and rheumatoid arthritis) and cancer [1]. Having numerous functions, these molecular scissors are meticulously controlled by mechanisms including regulation of gene expression, zymogen activation, post-translational modifications and through inhibition by different endogenous inhibitors. Based on physiological elements such as spatial and temporal localization, relative concentrations and binding parameters, two types of protease inhibitors exist: regulatory-type inhibitors and emergency-type inhibitors. Regulatory-type inhibitors offer local fine-tuned regulation of proteolysis. For instance, matrix metalloproteases (MMPs) are controlled by tissue inhibitors of metalloproteases (TIMPs). Emergency-type inhibitors reassure

rapid and broad inhibition of excess proteolysis [2], often by blocking circulating proteases in life-threatening conditions.

One protease inhibitor mainly known for its typical features of an emergency-type protease inhibitor is alpha-2-macroglobulin (α2M). This inhibitor comes with evolutionary ancestry, as it is also present in invertebrates [3]. In humans, this abundant plasma protein targets a broad range of proteases and is habitually considered a physiological guardian of broad-spectrum proteolysis [4, 5]. α2M is a 720 kDa glycoprotein with four identical subunits. Each subunit (180 kDa) contains a 'bait region', which is a stretch of approximately 25 amino acids functioning as an exceptionally good substrate for active proteases. Upon proteolysis of the bait region by active proteases, α2M becomes activated (α2M*) and undergoes a conformational change thereby physically 'trapping' the protease inside its cage-like structure (Fig. 1a) [6]. Next, α2M further reinforces this interaction by exposing a reactive thioester, which covalently binds accessible lysine residues from the activating protease (α2M*/protease) [7]. By covering the protease active site, α2M* prevents proteases to cleave large protease substrate molecules (e.g. gelatins), while the digestion of smaller molecules (e.g. peptides) remains possible [8]. Besides physically obstructing the interaction of proteases with their environment, α2M* simultaneously exposes receptor-binding domains (Fig. 1a). These domains interact with the scavenger receptor low-density lipoprotein receptor-related protein-1 (LRP-1) [9] or with GPR78 [10]. A main result of this process is the rapid clearance of α2M*/protease complexes from the circulation. In addition, under certain conditions, these complexes also mediate proliferation and migration of cancer cells [11], prostaglandin synthesis in macrophages [12, 13] and enhance CpG oligodeoxynucleotide-mediated stimulation of human peripheral blood mononuclear cells [14].

Due to the abundance of α2M in human plasma, several studies have been focused on the interaction between α2M and plasma proteases involved in hemostasis (e.g. thrombin and plasmin). Nevertheless, several recent studies have implicated α2M in pathologies of the nervous system. A2M mutations in the 'bait region' are associated with an increased risk for Alzheimer's disease [15] and cerebrospinal fluid levels of α2M are associated with neuronal injury in preclinical Alzheimer's disease [16]. Only a limited number of studies [17–20] have addressed the interaction between α2M and human MMPs, a family of zinc-dependent endopeptidases. Similar to α2M, MMPs are extracellular molecules with important roles in inflammation, cancer and vascular and neuronal diseases [21–23]. Due to their large substrate repertoire and involvement in several physiological processes, MMPs are subject to tight regulation and are secreted in the presence of an inhibitory pro-peptide domain (referred to as proMMP). Removal of the pro-peptide domain, also referred to as 'proMMP activation', is a prerequisite for MMP activity and the presence of a truncated protein band for activated MMP is often used as a marker for MMP activity [24, 25].

One MMP involved in both systemic and local pathologies is MMP-9 or gelatinase B [24, 26]. In healthy laboratory mice, bulk amounts of MMP-9 can be found in bone marrow, prestored in granules of neutrophils [27]. During an inflammatory insult or tissue damage, MMP-9 travels along with neutrophils to sites of infection or damage, where it further modulates processes, including tissue repair, wound healing and neoplasia [28]. For those reasons, MMP-9 is often analyzed in plasma or tissue samples of patients with (neuro)inflammation, immune disorders and cancer [24]. From both structural and biological perspectives, MMP-9 is unique. In comparison with other MMPs, MMP-9 has an extreme degree of flexibility due to the presence of a central *O*-glycosylated domain (Fig. 1b). This configuration allows independent movement of the N-terminal and C-terminal domains, and allows MMP-9 to 'crawl' along collagen fibrils in search for damaged regions [29–31]. Recently, we established that MMP-9 also forms circle-shaped covalently linked homotrimers which share a similar degree of flexibility (Fig. 1b). Most intriguingly, this stable homotrimeric form is produced simultaneously with monomeric MMP-9, both by human cell lines in vitro and retrieved in vivo (see Supplementary Figure S1a–d). Questioning why nature would simultaneously produce two protease forms, we wondered how these forms are regulated by the protease 'snap-trap' α2M. We first performed a detailed analysis of the interaction between α2M and MMP-9 mixtures and found that MMP-9 efficiently cleaves the α2M bait region, induces α2M conformational changes (α2M*) and forms covalent complexes (α2M*/MMP-9). In human plasma, active MMP-9 was efficiently complexed to α2M, resulting in a shift of active MMP-9 into high molecular weight complexes, only detectable by modified analysis for high-molecular weight proteases. When comparing MMP-9 monomers and trimers, we discovered that although both forms activate and bind α2M, α2M*/MMP-9 trimer complexes are subjected to reduced α2M anti-proteolytic activity, making the α2M*/MMP-9 monomer and α2M*/MMP-9 trimer complexes functionally completely different in nature. Finally, we also show that endocytosis of α2M*/MMP-9 trimer complexes is less efficient than α2M*/MMP-9 monomer complexes and hence escapes clearance from the extracellular environment.

Results

α2M is efficiently cleaved by MMP-9 mixtures

Since cleavage of the α2M bait region is the first step towards protease trapping, we examined whether active MMP-9 is able to cleave α2M. In vitro incubation of purified α2M with activated MMP-9 resulted in a single cut of

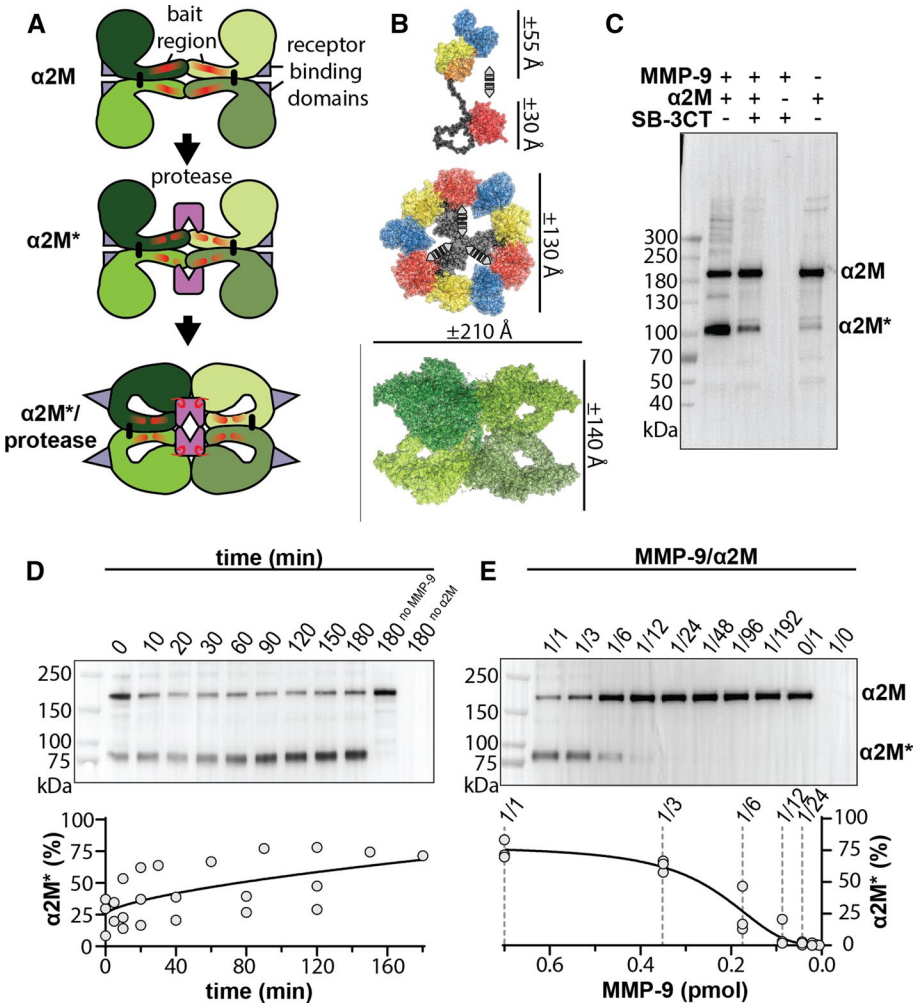

Fig. 1 α2M is efficiently cleaved by active MMP-9. **a** Illustration of the α2M inhibition mechanism. The tetrameric structure of α2M (±720 kDa) is formed by a non-covalent interaction between two covalently linked dimers (±360 kDa). Each individual monomer (±180 kDa) contains a protease bait region (red lines) and a buried receptor binding domain (gray triangles). Upon cleavage of the bait region, α2M becomes 'activated' (α2M*) and undergoes a conformational change. This results in physical trapping of the protease, the exposure of a reactive thioester bond which hooks to protease lysine residues (red hooks) and the surface exposure of the receptor binding domains for optimal clearance of α2M*/protease complexes from the circulation. **b** (Top panel) Structural model of an activated human MMP-9 monomer [29]. The active site (yellow), fibronectin repeats (blue), Zn^{2+}-binding domain (orange), *O*-glycosylated domain (black) and hemopexin domain (red) are shown. The gray arrowheads and lines symbolize the flexibility and relative distances between the active site and the hemopexin domains. (center panel) Structural model for activated trimeric MMP-9 [36]. The three gray symbols indicate the relative "swelling" of the MMP-9 trimer. (Bottom panel) Structure of activated human α2M* (PDB ID: 4AXQ) [6]. Each α2M monomer is shown in a different shade of green. **c**, Incubation of α2M with active MMP-9 (17 nM MMP-9/67 nM α2M) results in a single cut of α2M (α2M*) and the generation of ±90 kDa fragments. This process is reduced in the presence of an MMP-inhibitor (SB-3CT). **d** Cleavage of α2M by MMP-9 is fast (25% instant activation) and increases time-dependently (20 nM MMP-9/140 nM α2M). Relative quantification of three experiments (bottom panel). Y-axis indicates the percentage (%) of cleaved α2M. **e** Cleavage of α2M by MMP-9 (α2M at 140 nM with decreasing concentrations of MMP-9) requires a high α2M/MMP-9 ratio, likely due to the protease-inhibitory effect of the α2M/MMP-9 interaction. Relative quantification of three experiments (bottom panel). All images were obtained by Western-blot analysis under denaturing/reducing condition and detected with anti-α2M. *Y* axis indicates the percentage (%) of cleaved α2M. Quantification data were fitted with a four-parameter dose–response fit and are representative for three independent experiments (see Supplementary figure S2)

α2M (α2M*), splitting the molecule in halves with comparable sizes (±90 kDa) (Fig. 1c). The formation of α2M* was inhibited when adding the small-molecule MMP inhibitor SB-3CT and the natural inhibitor TIMP-1, indicating that MMP-9 proteolytic activity is required. In contrast, addition of the substrate-based peptide inhibitors CPU1 and CPU2 [32] only slightly inhibited α2M cleavage, suggesting that the α2M bait region is a highly efficient substrate which easily displaces substrate-based peptide inhibitors (Supplementary Figure S1e). The cleavage reaction was time-dependent

(Fig. 1d) and dose-dependent (Fig. 1e) and occurred almost instantly, with approximately 25% α2M* generated at time-point zero.

Active MMP-9 forms covalent complexes with α2M, detectable by modified in gel gelatin zymography analysis

Cleavage of the α2M bait region results in a large conformational change, physically "trapping" the protease and activating a buried cysteine–glutamine thioester bond which covalently interacts with free lysine residues [6, 7]. These conformational changes in α2M alter the molecule into a more compacted form or 'fast' form, which migrates faster during native PAGE analysis [33]. Indeed, interaction of MMP-9 with α2M, resulted in a 'fast' α2M* form during native electrophoresis (Fig. 2a). Moreover, under denaturing conditions, active MMP-9 in the presence of α2M resolved as minimum four high-molecular weight bands (Fig. 2b), a process which was both time-and dose-dependent, and followed a similar time-dependent and dose-dependent profile as the bait region cleavage experiments (Fig. 2d, e). These results indicate that MMP-9 and α2M are able to form covalent complexes (α2M*/MMP-9) likely through the interaction between the α2M reactive thioester and MMP-9 lysine chains [7]. The activated MMP-9 molecule (without the propeptide) contains 19 lysine residues (3.2% of all amino acids), which are located in the active site, fibronectin repeats, Zn^{2+}-binding domain and hemopexin domain (see Supplementary Figure S3a) and several of these are easily accessible (see Supplementary Figure S3b). Indeed, active MMP-9 mutants lacking the C-terminal hemopexin domain and the central *O*-glycosylated linker domain formed complexes with α2M with similar efficiency (see Supplementary Figure S3d, c), indicating that both intact and truncated MMP-9 forms are captured by α2M. Next, we wondered whether these complexes could be detected by gelatin zymography, a technique which is often applied

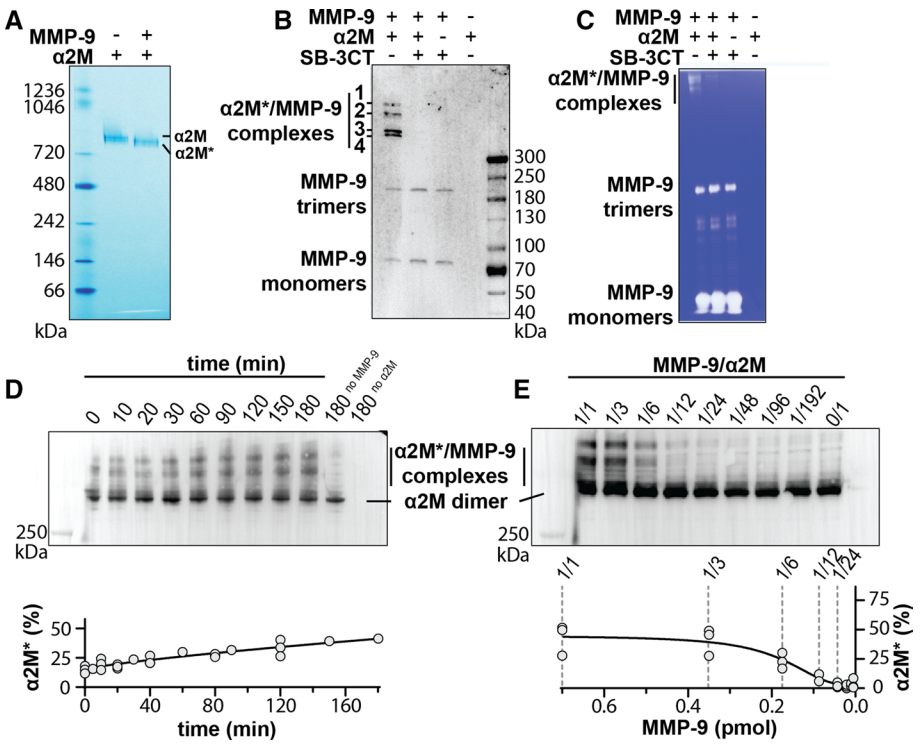

Fig. 2 Active MMP-9 is covalently trapped by α2M and presents as high-molecular weight complexes on gelatin zymograms. **a** MMP-9 converts native α2M into its electrophoretically 'fast' form (α2M*). Native electrophoresis with a protein ladder in the left lane for size standardization. Protein masses are indicated in kilodaltons (kDa). **b** Active MMP-9 forms four covalent complexes with α2M under denaturing conditions (Western blot analysis of MMP-9/α2M (17 nM/67 nM)) The presence of the MMP-inhibitor SB-3CT prevents the formation of these complexes. Proteins were separated under non-reducing conditions and visualized with an anti-MMP-9 antibody. **c** Covalent α2M*/MMP-9 (17 nM/67 nM) complexes are detected by modified gelatin zymography analysis. **d** The complex formation between α2M and MMP-9 (20 nM MMP-9/140 nM α2M) is time-dependent and occurs fast (±20% instant activation). Relative quantification of three experiments (bottom panel). **e** Formation α2M*/MMP-9 complexes is dose-dependent (α2M at 140 nM with decreasing concentrations of MMP-9) and requires a high α2M/MMP-9 ratio. Relative quantification of three experiments (bottom panel). **d**, **e** Western-blot analysis under non-reducing conditions and detected with an anti-α2M antibody. Quantification data were fitted with a four-parameter dose–response fit and are representative for three independent experiments (see Supplementary figure S2)

to analyze the presence of MMP-9 proteoforms and activation status in biological samples [25]. After modification of the standard gelatin zymography protocol for the detection of high-molecular weight complexes, α2M*/MMP-9 complexes were indeed detected (Fig. 2c).

MMP-9 efficiently cleaves α2M and forms covalent complexes in human plasma

A2M is secreted by the liver into the blood circulation and forms a prominent component of human plasma [34]. We hypothesized that in human plasma, activated MMP-9 will also cleave α2M and form high-molecular weight covalent complexes. Indeed, when added to human plasma, activated MMP-9 efficiently generated the ± 90 kDa α2M* cleavage fragment (Fig. 3a). Equally so, a similar pattern of four α2M*/MMP-9 complexes was seen after non-reducing SDS-PAGE and immunoblot analysis (Fig. 3b). For further experiments, we defined the complexes between α2M and MMP-9 with the numbers 1–4. With these results, we confirmed cleavage by MMP-9 and complex formation between MMP-9 and α2M in a biologically relevant setting, namely human plasma. Interestingly, addition of activated MMP-9 to human plasma also resulted in the complete disappearance of activated MMP-9 and conversion into α2M*/MMP-9 complexes. This effect was also visible by modified gelatin zymography analysis (Fig. 3c) and yields a completely new interpretation for zymography analysis.

Detection of activated MMP-9 in human plasma is masked by α2M complex formation

Since MMP-9 is implicated in a wide range of human diseases [24], researchers regularly analyze the presence of

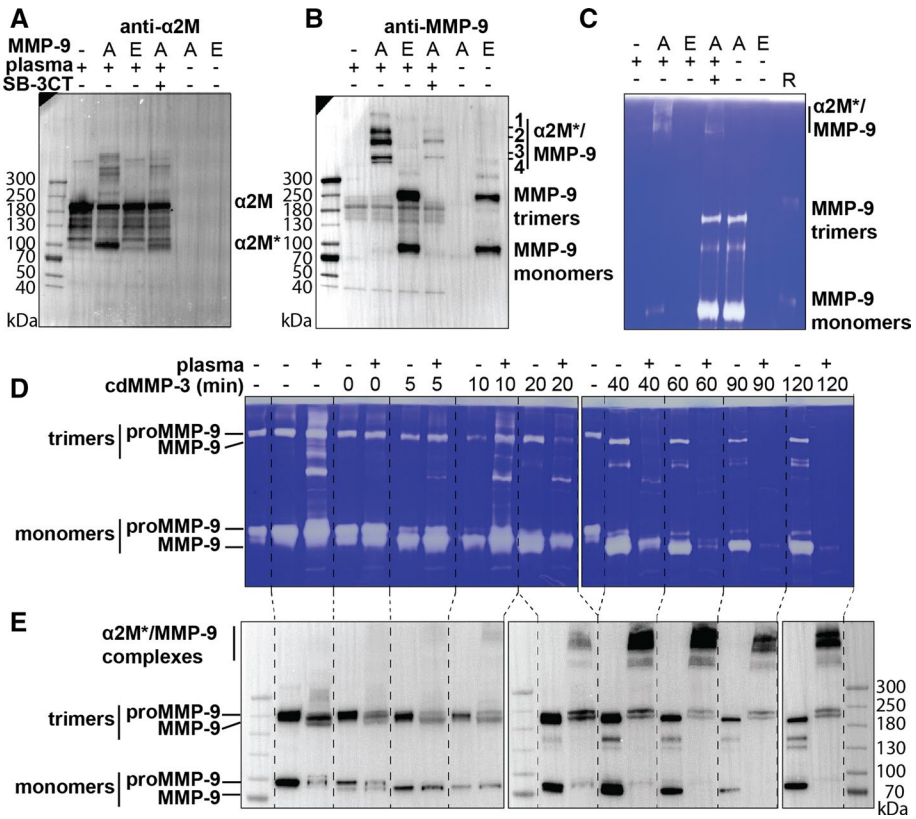

Fig. 3 Active MMP-9 efficiently cleaves and complexes α2M in human plasma. **a** In human plasma, activated MMP-9 (A) cleaves α2M (0.5 pmol MMP-9/µl plasma) with a single cut, splitting the molecule in halves with comparable sizes (α2M*). This process is reduces in the presence of the MMP inhibitor SB-3CT and does not occur with an inactive MMP-9 mutant (E). Images represent an SDS-PAGE analysis (reducing conditions) followed by Western blot with an anti-α2M antibody. **b** Activated MMP-9 (A) forms four covalent complexes with α2M in human plasma. This process is reduced in the presence of the MMP inhibitor SB-3CT and does not occur with an inactive MMP-9 mutant (E). Images represent an SDS-PAGE analysis (non-reducing conditions) followed by Western blot analysis (anti-MMP-9 antibody). **c** The formation of α2M*/MMP-9 complexes in human plasma is detected by modified gelatin zymography analysis. Images in panels A-C are representative of 3 experiments with plasma from three different plasma donors (see Supplementary Figure S4). **d**, **e** Gradual activation of proMMP-9 was induced by addition of the catalytic domain of MMP-3 (cdMMP-3). In the presence of human plasma, fully activated (± 80 kDa) MMP-9 was efficiently converted into high-molecular weight complexes, undetectable by standard gelatin zymography analysis. **d** Standard gelatin zymography analysis. **e** Western-blot analysis with anti-MMP-9 (AB6008)

MMP-9 in human plasma samples. Given the excessive presence of α2M in human plasma (> 1.5 mg/ml plasma from healthy donors [34, 35]), we hypothesize that in plasma samples, the presence of activated MMP-9 goes undetected by complex formation with α2M. To evaluate the extent of this phenomenon, we investigated the 'disappearance' of the band for activated MMP-9. Incubation of proMMP-9 with the catalytic domain of MMP-3 (cdMMP-3) resulted in a step-wise removal of the self-inhibitory propeptide domain and the appearance of a ± 82 kDa band of activated MMP-9 (full activation after 2 h) (Fig. 3d, e). Depending on the activation status, addition of human plasma resulted in the disappearance of the gelatinolytic band of fully activated MMP-9 on standard gelatin zymograms (Fig. 3d). This effect was due to the conversion of active MMP-9 into a high molecular weight MMP-9/α2M complex which we detected by Western-blot analysis for high-molecular weight proteins (Fig. 3e). This effect was highly efficient (± 5 min reaction time) and completely converted all activated MMP-9 into the high molecular weight α2M*/MMP-9 complexes without any saturation, even above physiological MMP-9 concentrations (> 1 nM). Besides reinterpretations of all previous literature on plasma MMP-9 monomers, our methodological modifications made it possible to detect what was previously not seen and enabled us to tackle the question whether differences exist between monomers and trimers of MMP-9 bound to α2M.

Trimeric MMP-9 is less sensitive to α2M antiproteolytic activity

Whereas most MMP-9 (± 70%) is produced as monomeric proteases, approximately 30% is secreted as stable homotrimers. Previously, we found that trimeric MMP-9 is more sensitive to TIMP-1 inhibition during the induction of angiogenesis [36]. Therefore, and in view of the considerable size differences (Fig. 1b), we questioned whether MMP-9 monomers and trimers interact differently with the systemic protease inhibitor α2M. As a first test, we analyzed the sensitivity of gelatinolysis by active MMP-9 monomers, trimers and their mixture (30% trimers) to inhibition by purified α2M (Fig. 4a, and Table 1). Interestingly, monomeric MMP-9 was approximately five times more sensitive to α2M inhibition compared to trimeric MMP-9 and this result was corroborated with human plasma from different donors (Fig. 4b). Statistical comparisons of the best-fit IC50 values (extra sum-of-squares *F* test) confirmed that the residual inhibitory activities of purified α2M and human plasma were significantly different ($p < 0.0001$) for each dataset. In addition, remaining gelatinolytic activity associated with MMP-9 trimers could be further inhibited by addition of TIMP-1 (Supplementary Figure S6a).

Monomeric and trimeric MMP-9 cleave and bind to α2M equally well

Since the first interaction between MMP-9 and α2M relies on cleavage of the α2M bait region, we hypothesized that the larger trimeric MMP-9 form might have less access to the α2M bait region than monomeric MMP-9. Interestingly, both MMP-9 proteoforms equally well generated the cleaved α2M* fragments, both with purified human α2M and in human plasma (Fig. 4c). Statistical analysis of three independent experiments of the dose- and time-dependent cleavage of α2M indeed revealed no significant differences between monomers, trimers and their mixtures (Fig. 4e, f). Analysis of complex formation between α2M monomers and trimers revealed that α2M*/MMP-9 complexes 2 and 4 are formed by α2M*/MMP-9 monomers and complexes 1 and 3 are α2M*/MMP-9 trimers, as seen both by Western blot analysis and gelatin zymography (Fig. 4d). The numbers 1–4 refer to the complexes defined in Fig. 3b. However, no differences in complex formation efficiency were observed (Fig. 4g, h).

Trimeric MMP-9 bound to plasma α2M remains catalytically active

Given the relatively large size of trimeric MMP-9 compared to α2M (Fig. 1b), it is difficult to imagine how trimeric MMP-9 is fully trapped within the α2M cage. Therefore, we hypothesized that trimeric MMP-9 might remain (partially) active outside of the α2M cage (Fig. 5a). To investigate the molecular dimensions of the native complexes, we compared α2M*/MMP-9 monomer and α2M*/MMP-9 trimer complexes by native electrophoresis (Fig. 5b). As shown in Fig. 2a, active MMP-9 converted α2M in a 'fast' form (α2M*) by inducing a conformational change with more compact properties. Interestingly, trimer-induced α2M* also resulted in a slower form (α2M*tri) which also occurred with MMP-9 mixtures. This suggests that MMP-9 trimers can form a more 'bulky' complex. Since both MMP-9 monomers and trimers are flexible molecules [30, 31, 36], we hypothesized that one of the three active sites in trimeric MMP-9 might cleave and bind α2M, while the remaining active sites remain active. To investigate this hypothesis, active MMP-9 monomers, trimers or their mixtures, were allowed to bind purified α2M and these complexes were immobilized on anti-α2M-coated beads. After thorough washing to remove the excess of MMP-9, the bead-bound complexes were incubated with fluorogenic gelatin to detect α2M-associated proteolysis. Interestingly, α2M*/MMP-9 trimer complexes retained significantly more proteolytic activity than α2M*/MMP-9 monomers (Fig. 5c). In a similar set-up, we investigated the activity retained in α2M*/MMP-9 complexes formed by reaction of human plasma

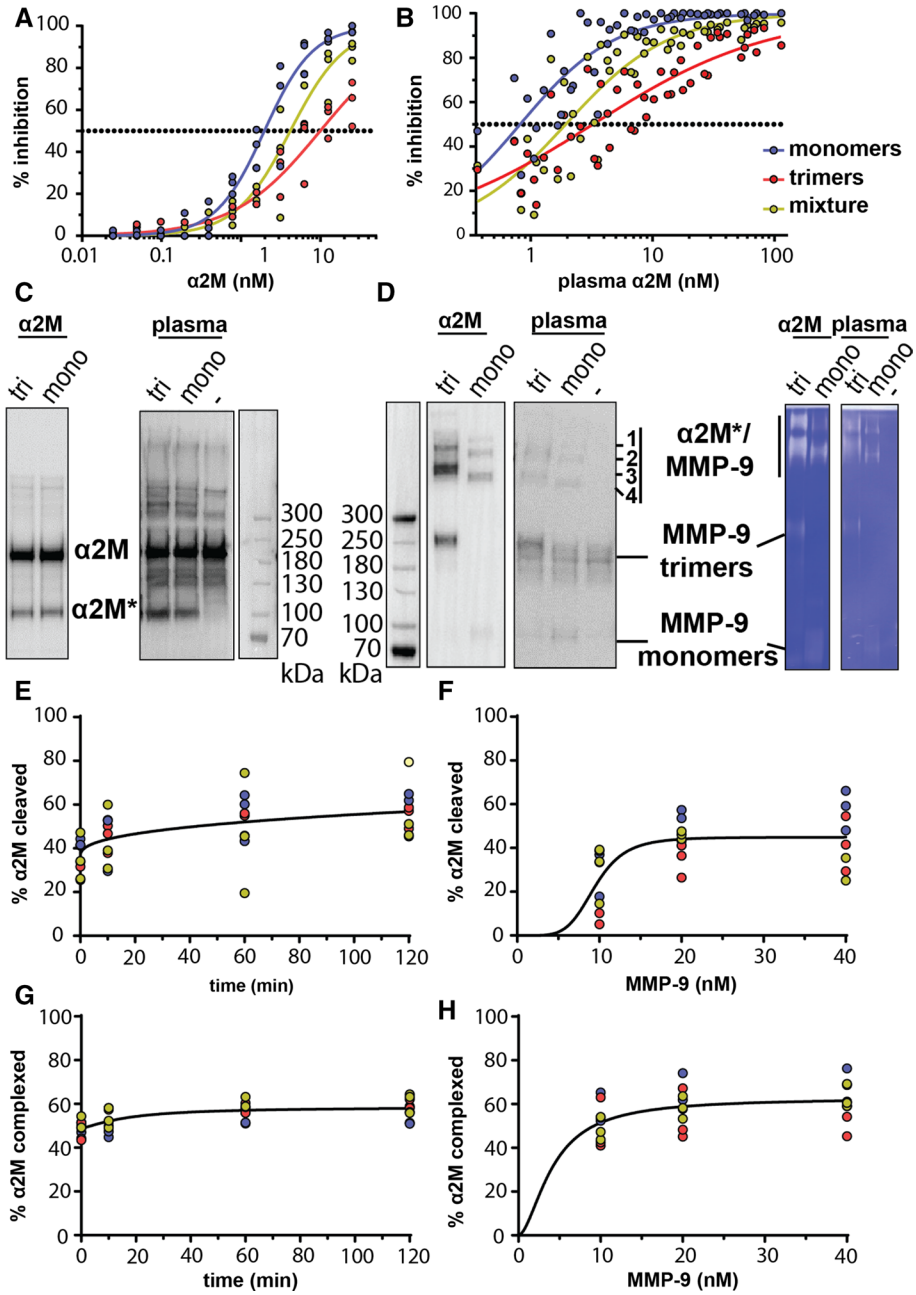

Fig. 4 Inhibition and interaction of α2M with monomeric and trimeric MMP-9. **a** The degradation of gelatin by active MMP-9 monomers (blue) was more efficiently inhibited by purified α2M in comparisons with MMP-9 trimers (red) and their mixtures (yellow). Data fitted with a standard dose–response fit, $n=3$ (each from an independent experiment). **b** The degradation of gelatin by active MMP-9 monomers (blue) was more efficiently inhibited by human plasma in comparisons with MMP-9 trimers (red) and their mixtures (yellow). Data fitted with a standard dose–response fit, $n=7$ (7 plasma samples from different donors, analyzed in three independent experiments). **c** both MMP-9 monomers and trimers cleave α2M (purified α2M and human plasma) with a single cut, splitting the molecule in halves with comparable sizes (α2M*). Images represent SDS-PAGE analysis (reducing conditions) followed by Western blot analysis (anti-α2M antibody). **d** MMP-9 monomers and trimers form complexes with α2M representing, respectively, complexes 2 and 4 and complexes 1 and 3. This effect is seen with purified α2M and in human plasma. Images on the left represent SDS-PAGE analysis (non-reducing conditions) followed by Western blot analysis (anti-MMP-9 antibody). Images on the right represent modified gelatin zymography analysis (33 nM MMP-9/333 nM α2M or 0.5 µl plasma per pmol MMP-9). **e** MMP-9 monomers and trimers (20 nM MMP-9/140 nM α2M) cleave α2M equally well in a time-dependent manner. **f** MMP-9 monomers and trimers equally well digest α2M in a dose-dependent manner (α2M at 140 nM with decreasing concentrations of MMP-9). **g** The profile of complex formation between α2M and MMP-9 monomers and trimers (20 nM MMP-9/140 nM α2M) is similar over time. **h** The complex formation between α2M and MMP-9 monomers/trimers is comparable across different doses. Panels E–H represent relative quantifications of Western-blot images of three independent experiments. Data were not significantly different as confirmed by extra sum-of-squares F test and fitted by one joint four-parameter dose-response fit (black). See Supplementary Figure S5 for associated Western-blot images

Table 1 Inhibitory capacity of purified α2M and human plasma on gelatinolysis by MMP-9 monomers and trimers

	MMP-9 monomers	MMP-9 trimers	MMP-9 mixture[a]
Purified α2M			
IC50 (CI)	1.97 (1.67–2.33) nM	9.94 (7.98–12.73) nM	4.18 (3.43–5.09) nM
R^2	0.959	0.918	0.931
n	3	3	3
Human plasma			
IC50 (CI)	0.82 (0.57–1.06) nM	3.24 (2.38–4.24) nM	1.94 (1.49–2.43) nM
R^2	0.713	0.753	0.765
n	7	7	7

Half-maximal inhibitory concentration (IC50), reported as best-fit value and 95% confidence interval (CI)

R^2 goodness of dose–response fit, *n* number of experiments

[a]MMP-9 mixture consists of approximately 70% monomers and 30% trimers [36]

with MMP-9 monomers, trimers and their mixtures. Again, α2M*/MMP-9 trimers retained significantly more activity than α2M*/MMP-9 monomers (Fig. 5d), illustrating the biological relevance of our findings. In addition, we also confirmed our data with MMP-9 purified from human neutrophils (Supplementary Figure S6e). Finally, we also showed that the remaining α2M-associated proteolytic activity could be neutralized by excess amounts of α2M (5 µM α2M) indicating that α2M*/MMP-9 trimer activity might be overcome in conditions with high α2M concentrations (Supplementary Figure S6f).

α2M*/MMP-9 trimer complexes escape clearance through LRP-1 receptor-mediated endocytosis

α2M*/protease complexes are efficiently cleared from the circulation or extracellular space through receptor-mediated endocytosis [37]. To evaluate whether α2M*/MMP-9 complexes are cleared from the extracellular environment, we investigated LRP-1-mediated uptake by the U-87 cell line (glioblastoma cell line which expresses considerable amounts of the α2M-receptor LRP-1). α2M was labeled with a pH-sensitive dye which fluoresces in acidic environments such as endosomes. Labeling of α2M did not interfere with the interaction between α2M and MMP-9 (Supplementary Figure S7a). Furthermore, α2M challenged with active MMP-9 (α2M*/MMP-9 complex formation), resulted in a significantly better uptake compared to intact α2M and appearance of the fluorescent signal in intracellular vesicles (Supplementary Figure S7b, c). Interestingly, α2M*/MMP-9 trimer complexes were significantly less endocytosed compared to α2M*/MMP-9 monomer complexes (Fig. 5e, f). Mixtures of α2M*/MMP-9 trimer and α2M*/MMP-9 monomer complexes also underwent reduced endocytosis compared to α2M*/MMP-9 monomer complexes alone, suggesting that the presence of α2M*/MMP-9 trimer complexes affects total clearance. Internalization of the LRP-1 receptor was also confirmed by flow cytometry analysis (Fig. 5g). As expected, separate addition of α2M, MMP-9 monomers or MMP-9 trimers resulted in a reduction of cell surface fluorescence associated with LRP-1, since endocytosis of free MMP-9 has also been reported [29]. However, cells treated with α2M*/MMP-9 monomers had a further reduced signal for cell surface LRP-1 compared to α2M or α2M*/MMP-9 trimers. α2M*/MMP-9 trimer complexes are thus able to avoid clearance by LRP-1 receptor-mediated endocytosis.

Discussion

α2M is a general protease check-point in human physiology. With concentrations higher than 1.5 mg/ml in the circulation of healthy individuals [34], plasma α2M efficiently controls active proteases by first limiting their contact with potential substrates, followed by providing a vehicle for rapid receptor-mediated clearance from the extracellular environment [5]. Whereas the interaction between α2M and common systemic serine proteases has extensively been investigated [38, 39], little is known about α2M interactions with MMPs. Similar to α2M, MMPs are secreted proteins with a wide range of functions in biology and pathology, including in sepsis/endotoxin shock [40], neurological disease [26, 41], wound healing [42, 43] and cancer, making these proteases ideal interaction partners. To better understand the regulation of MMPs by α2M, we investigated the interaction between MMP-9, one of the most studied MMPs [24], and α2M.

We found that the general interaction mechanism between active MMP-9 and α2M is similar to that described for other proteases. MMP-9 (both monomeric and trimeric forms) efficiently cleaves the α2M bait region, resulting in α2M activation and the formation of a covalent interaction (α2M*/MMP-9). Indeed, the formation of a covalent complex between MMP-9 (mixtures) and α2M is mentioned in the literature, but never further elaborated on [44]. Interestingly, active MMP-9 (as high as ± 250 nM) is entirely complexed

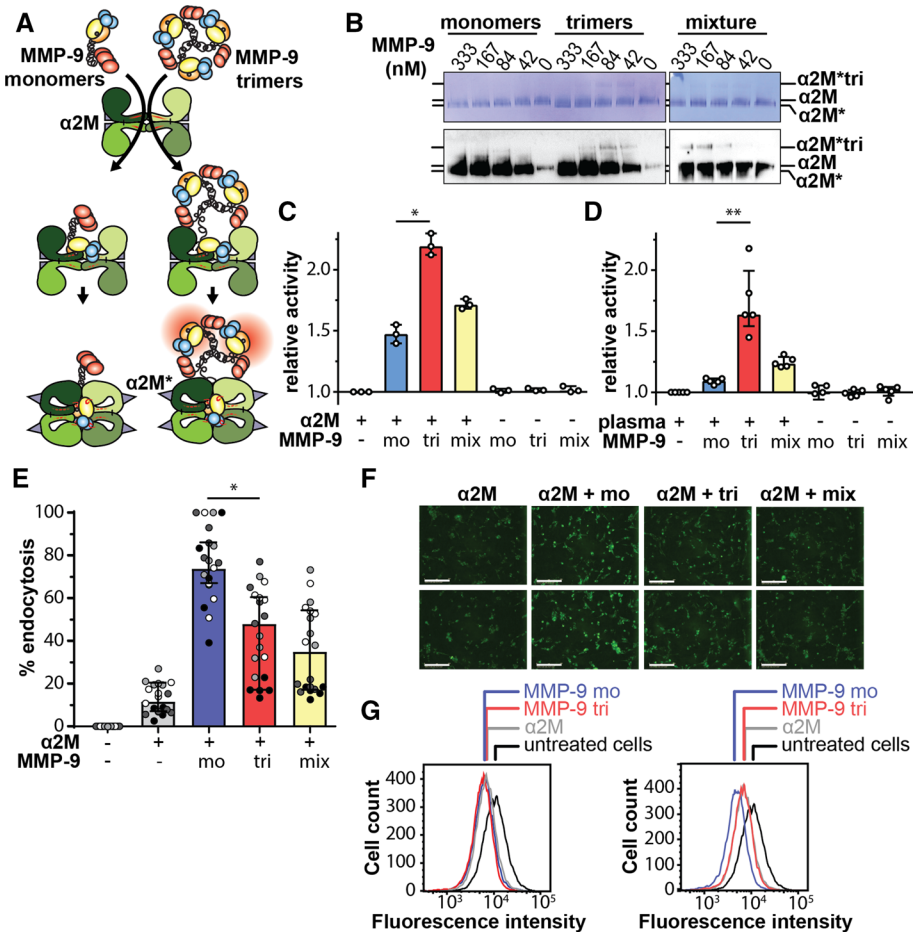

Fig. 5 α2M*/MMP-9 trimer complexes remain partially active and escape LRP-1-mediated endocytosis. **a** Proposed model for the interaction between active MMP-9 monomers/trimers and α2M. Given the size and flexibility of MMP-9 trimers, protease active sites remain exposed in the environment and travel as proteolytically active proteases linked to α2M. **b** Native PAGE analysis of α2M*/MMP-9 complexes reveals the existence of a slower form in samples containing MMP-9 trimers (α2M*tri) (666 nM α2M with a ½ dilution of MMP-9 monomers, trimers or their mixture). Top, Coomassie blue stained native PAGE gel. Bottom, Western-blot analysis with an anti-α2M antibody. See Supplementary Figure S6 for repeat experiments. **c** α2M*/MMP-9 trimer complexes immobilized on anti-α2M beads retain a significant amount of their proteolytic activity against gelatins. Each data point represents an independent experiment ($n=3$). Relative activities represent the fold change in fluorescence compared to α2M alone (background signal). **d** α2M*/MMP-9 trimer complexes from human plasma, immobilized on anti-α2M beads, retain a significant amount of their proteolytic activity against gelatins. Relative activities represent the fold change in fluorescence compared to α2M alone. Each data point represents an independent experiment ($n=5$). $^{*}p<0.05$, $^{**}p<0.01$, as determined by Kruskal–Wallis test with Dunn's correction for multiple comparisons. Bars represent median values with indication of the interquartile range as error bars. **e,** The relative amounts of α2M*/MMP-9 monomers found in endocytic vesicles are significantly increased compared to α2M*/MMP-9 trimers. Data represent four independent experiments, with each experimental replicates shown in the same color. Bars represent mean values. Data were normalized to the highest value in each experiment. $^{*}p<0.05$, as determined by Mann–Whitney test on the mean values of each experiment. **f** Representative images of α2M endocytosis. Bright green fluorescence represents the uptake of pH-rhodo-labeled α2M complexes and presence in acidic vesicles. Size bars indicate 200 µm. **g** Flow cytometry analysis of U-87 cells for the presence of cell surface LRP-1 when treated with combinations of α2M and MMP-9 proteoforms. α2M, MMP-9 monomers and MMP-9 trimers reduce the amount of LRP-1 present on cell surfaces. Complexation of α2M to MMP-9 monomers results in an additional reduction in comparison with MMP-9 trimers indicating more LRP-1 internalization and endocytosis. Data are representative for two independent experiments (See Supplementary Figure S7 for repeat experiments)

to α2M within 5 min. While MMP-9 concentrations in the blood of healthy individuals approximate 650 pM, in conditions with high MMP-9 blood levels (e.g. severe sepsis) MMP-9 only increases up to 1 nM [45]. Therefore, we believe that any activated MMP-9 released in the circulation is efficiently complexed to α2M. Moreover, the complex formation between MMP-9 and α2M results in complete disappearance of the protein bands for activated MMP-9 monomers and trimers on both standard gelatin zymograms and Western blot images. α2M*/MMP-9 complex formation thus masks active MMP-9 in human plasma and prevents its detection by the most frequently used analysis techniques.

While many studies have selected circulating levels of MMP-9 as a diagnostic or predictive disease marker (e.g. in cardiovascular diseases [46–48], autoimmune diseases [49] and cancer [50]), our study strongly advocates the analysis of high-molecular weight α2M*/MMP-9 complexes as a novel measure for MMP-9 activation.

Whereas the active sites of MMP-9 monomers are efficiently trapped by α2M and thereby shielded from cleaving large substrates (e.g. gelatins), we show that MMP-9 trimers retain some proteolytic activity against large substrates when complexed to α2M*. MMP-9 trimers are thus less sensitive to direct inhibition by α2M, yet, monomeric and trimeric MMP-9 equally well cleave α2M and form covalent complexes. Looking at the molecular dimensions of α2M and MMP-9 monomers and trimers (Fig. 1b), one MMP-9 active site (and possibly also the hemopexin domain) might fit within the cage of activated α2M. In addition, both MMP-9 monomers [30] and trimers [36] are highly flexible in nature. In our proposed model (Fig. 5a), the flexibility of the central *O*-glycosylated domain allows trimeric MMP-9 to become partially trapped within the α2M cage, while some active sites remain exposed to the environment, explaining the significantly higher residual activity of α2M*/MMP-9 trimers in comparison with α2M*/MMP-9 monomers. Furthermore, the free active sites in the α2M*/MMP-9 trimer complexes can still be inhibited in the presence of excessive amounts of α2M such as found in human plasma (5 μM). Hence, the physiological relevance of α2M*/MMP-9 trimer complexes is likely to be most pronounced in tissues or at sites of local inflammation where invading neutrophils release bulk amounts of TIMP-free MMP-9 [27].

A second level of protease regulation by α2M is by tagging α2M*/protease complexes for efficient removal from the extracellular environment through LRP-1-mediated endocytosis [5]. Here, we showed that through homotrimerization, MMP-9 delays its clearance. Whereas α2M*/MMP-9 monomer complexes were efficiently taken up by LRP-1-mediated endocytosis, α2M*/MMP-9 trimer complexes showed reduced endocytosis. This partially resolves the enigma why in nature two different forms of MMP-9 co-exist. Indeed, both proteoforms are endowed with different functions in the presence of local TIMP-1 [36] or the emergency inhibitor α2M in plasma.

In conclusion, our insights help to understand how different MMP-9 proteoforms behave within the complex environments of the emergency-type protease inhibitor α2M. Natural MMP-9 exists in two forms: on average 70% monomers and 30% trimers [36]. This redundancy is not superfluous as the catalytic action of the monomers is inhibited, whereas proteolysis by the trimers persists. Furthermore, this difference also translates into a reduced clearance of MMP-9 trimers from the extracellular environment. Finally, we caution about the interpretation of data obtained for standard analyses of (pro)MMP-9 in human plasma. By complex formation to α2M, active MMP-9 exclusively disappears into high-molecular weight α2M*/MMP-9 complexes. Another medical consequence is that in plasma-rich exudates, for instance occurring in acute and chronic wounds, detrimental MMP-9 activity may persist thanks to the α2M*/MMP-9 trimer complexes.

Experimental procedures

Proteins, reagents and buffers

Full-length human proMMP-9, a catalytically dead Glu^{402} to Ala^{402} mutant (proMMP-9 MutE), a mutant lacking the hemopexin domain (proMMP-9 ΔHem), a mutant lacking the *O*-glycosylated domain (proMMP-9 ΔOG) and a mutant lacking both the hemopexin and *O*-glycosylated domains (proMMP-9 ΔOGΔHem) were expressed in Sf9 cells and purified by gelatin-sepharose chromatography as previously described [29]. Stable full-length proMMP-9 monomers and trimers were separated by glycerol gradient ultracentrifugation as previously described [36] (see Supplementary Figure S1). ProMMP-9 mixture and the separated monomers and trimers were activated by incubation with the catalytic domain of MMP-3 (cdMMP-3, cat. No. 444217, Merck Millipore, Darmstadt, Germany) as previously described [29]. Activation of proMMP-9 was confirmed by a band shift of approximately 10 kDa, corresponding to the removal of the propeptide domain and by detection of gelatinolytic activity with a previously described gelatin degradation assay [51]. α2M purified from human plasma was purchased from Sigma Aldrich (Cat. No. M6159). Human plasma samples were collected from healthy volunteers who gave written informed consent in accordance with the Declaration of Helsinki. Plasma concentrations of α2M were determined using a DuoSet ELISA (DY1938, R&D Systems, Minneapolis, MN, USA).

SDS-PAGE, native PAGE and Western blot analysis

For SDS-PAGE analysis under reducing conditions (e.g. detection of cleaved α2M or α2M*), samples were prepared in reducing loading dye (125 mM Tris/HCl pH 6.8, 10% β-mercaptoethanol, 4% SDS, 20% glycerol, 0.1% bromophenol blue) and boiled for 20 min prior to electrophoresis. For non-reducing conditions, samples were prepared in non-reducing loading dye (125 mM Tris/HCl pH 6.8, 2% SDS, 20% glycerol, 0.1% bromophenol blue) without boiling. Proteins were separated on 4-12% Novex Tris–glycine gels in a mini gel tank as instructed by the supplier (Invitrogen, Carlsbad, CA, USA). For native analysis of α2M/MMP-9 complexes, samples were separated on native PAGE

3–12% bis–tris protein gels (Invitrogen, Carlsbad, CA, USA) using a blue native PAGE setup as described by the supplier. Transfer of proteins to PVDF membranes was done with the Trans-Blot Turbo Transfer System (Biorad, Hercules, CA, USA). Next, membranes were blocked for 1 h in 5% BSA with TBST buffer (150 mM NaCl, 0.1% Tween 20, 50 mM Tris, pH 7.5) and incubated overnight with goat anti-human α2M (AF1938, R&D Systems, Minneapolis, MN, USA), mouse anti-human MMP-9 (REGA-2D9, made in-house as previously described [52]) or rabbit anti-human MMP-9 (AB6008, Merck Millipore, Darmstadt, Germany). After washing, the blot was incubated with peroxidase-conjugated anti-goat IgG (PI-9500, Vector Labs, Burlingame, CA, USA), anti-mouse IgG (115-035-071, Jackson ImmunoResearch, Cambridgeshire, UK) or anti-rabbit IgG (711-035-152, Jackson ImmunoResearch, Cambridgeshire, UK) for 1 h at room temperature. Finally, Western blots were imaged using the Vilber Lourmat Fusion system (Labtech International, Heathfield, TN, USA) and Pierce ECL Western Blotting Substrate (Thermo Fisher Scientific, Waltham, MA, USA).

Standard and modified gelatin zymography

Standard gelatin zymography gels were 8 cm long and had a thickness of 0.75 mm. The separating gel consisted of 7.5% acrylamide/bis-acrylamide (cat. No. 1610146, Bio-Rad, Hercules, CA, USA) with 1 mg/ml gelatin (cat. No. G-1890, Sigma-Aldrich, St. Louis, MO, USA) in 0.1% SDS and Tris/HCl pH 8.8. Modified gelatin zymography gels were optimized for the detection of high-molecular weight MMP-9 complexes (> 250 kDa). The gels were 10 cm long, 0.75 mm thick and the running gel consisted of 6% ProSieve™ 50 Acrylamide (cat. No. 50617, Lonza, Bazel, Zwitserland) with 1 mg/ml gelatin, 0.1% SDS and 1.875 M Tris/HCl pH 8.8. Separating gels were topped with a 5% stacking gel in Tris/HCl pH 6.8. Gels were placed in an electrophoresis system buffered with 25 mM Tris, 192 mM glycine, 0.1% SDS. After electrophoretic separation, the gels were washed twice for 20 min in re-activation solution (2.5% Triton-X-100). Next, the gel was incubated overnight in 50 mM Tris–HCl, 10 mM $CaCl_2$ pH 7.5 at 37 °C. Staining was performed with 0.1% Coomassie Brilliant Blue R-350 (GE Healthcare). Western blots and zymograms were quantified with the ImageQuant TL software (GE Healthcare).

Incubation conditions

Unless mentioned otherwise, all incubations were done at 37 °C for 1 h in assay buffer (150 mM NaCl, 5 mM $CaCl_2$, 0.01% Tween-20, 50 mM Tris, pH 7.4) in a ThermoMixer (ThermoMixer C, Eppendorf). For comparisons of different MMP-9 forms, samples were first equilibrated based on gelatin degradation activity. MMP-9 and A2M concentrations vary and are specified in the figure legend of each experiment. SB-3CT (sc-205847, Santa-Cruz Biotechnology, Dallas, USA) was used at a concentration of 300 µM. To determine the uptake of MMP-3-activated MMP-9 in human plasma, proMMP-9 (10 µM) was incubated with cdMMP-3 (0.1 µM) at 37 °C. From this mixture, samples (0.2 µl) were taken at 0–120 min and either incubated for 5 min with human plasma (8 µl) or assay buffer. The reaction was stopped by adding 10 µl non-reducing loading buffer.

Gelatin degradation assay and on-bead gelatinolysis

To determine the inhibitory effect of α2M on MMP-9 activity, we used a previously described gelatin degradation assay [51]. To determine the activity of captured MMP-9 forms, α2M and MMP-9/α2M (42 nM MMP-9/70 nM α2M) or MMP-9/plasma (42 nM MMP-9/2.5 µl plasma in 10 µl total volume) incubations (1 h at 37 °C) were immobilized on anti-human α2M (AF1938, R&D Systems, Minneapolis, MN, USA) conjugated to Protein G Dynabeads (Immunoprecipitation kit, cat. No. 10007D, Thermo Fisher Scientific, Waltham, MA, USA). After three washing steps in washing buffer, the bead-α2M-complexes were transferred to a new tube and washed once more with assay buffer (150 mM NaCl, 5 mM $CaCl_2$, 0.01% Tween-20, 50 mM Tris, pH 7.4). Next, Dye-quenched gelatin (DQ™-gelatin, Invitrogen, Carlsbad, CA, USA) at a concentration of 2.5 µg/ml was added to the beads, and this mixture was placed at 37 °C in a ThermoMixer (ThermoMixer C, Eppendorf), shaking at 300 rpm. After 90 min (incubation with purified α2M) or 120 min (incubation with human plasma), gelatin degradation was measured in the supernatant equivalent to the fluorescence intensity (ex. 485 nm/em. 530 nm) as a readout, measured with the CLARIOstar microplate reader (BMG Labtech, Ortenberg, Germany).

Cell culture, live cell imaging and flow cytometry

U-87 cells were grown in DMEM with 10% fetal calf serum (FCS) and used between passages 2 and 10. To track endocytosis of α2M/MMP-9 complexes, α2M was labeled with pHrodo Green (pHrodo green STP ester, Invitrogen, Carlsbad, CA, USA) and purified from free label using dye removal columns (Invitrogen, Carlsbad, CA, USA). For live cell imaging of α2M endocytosis, U-87 were grown in 96-well plates and prior to imaging, growth medium was replaced with serum-free DMEM optimized for live-cell fluorescence microscopy (FluoroBrite™ DMEM, Invitrogen, Carlsbad, CA, USA). Next, labeled α2M or α2M/MMP-9 complexes were added at the equivalent of 10 nM α2M per condition and uptake was followed using the Incucyte

live-cell analysis system (Essen BioScience, Hertfordshire, UK). Values for relative endocytosis were calculated by dividing the amount of green signal (green channel area) by the total cell surface (cell confluence area). Values for time-point 0 h were subtracted and to allow comparison of data from four independent experiments, data from each experiment were normalized to the highest value and expressed as percentage endocytosis. Graphs and images shown represent conditions at 6 h after addition of α2M or α2M/MMP-9 complexes. For flow cytometry analysis of the LRP-1 receptor, U-87 cells were grown to confluence in T25 flasks, washed with phosphate-buffered saline (PBS), and α2M or α2M/MMP-9 complexes (at a concentration equivalent to 1 nM α2M) were added in FluoroBrite DMEM. After 3 h, cells were dissociated from cell culture flasks using enzyme-free cell dissociation buffer (Gibco/Thermofisher, Waltham, MA, USA), and incubated with FcR-block (Miltenyi Biotec) for 15 min on ice. Cells were stained with the Zombie Aqua™ Fixable Viability Kit (Biolegend, San Diego, CA, USA) and with PE-conjugated anti-LRP-1 (cat. no. 12-0919-42, eBioscience/Thermofisher, Waltham, MA, USA). Cells were run on an LSRFortessa X20 (BD Biosciences) equipped with DIVA software and analyzed with the FlowJo software (LLC, V10, Ashland, OR, USA). Forward and side scatter analysis was used to limit debris and doublets. Dead cells were excluded from the analysis based on Zombie Aqua™ staining.

Statistics and data processing

Graphs, data fitting, normalizations and statistics were performed with the GraphPad Prism software and detailed information on the statistical methods used is mentioned in the figure legends of the associated figures. Multi-panel figures were composed using the Adobe Illustrator CC 2018.

Acknowledgements The authors would like to thank Erik Martens, Karen Turneer, Jens Van Bael and Michael Van Canneyt for their assistance with the zymography analysis and the separation of MMP-9 monomers and trimers. EUB and JV are postdoctoral fellows funded by the Rega Foundation and the Research Foundation of Flanders (FWO-Vlaanderen). Project funding was from KU Leuven through a C1 grant (C16/17/010), the Belgian Charcot Foundation and FWO-Vlaanderen (Grants G0A7516N and G0A5716N).

References

1. Seife C (1997) Blunting nature's Swiss army knife. Science 277(5332):1602–1603
2. Turk B (2006) Targeting proteases: successes, failures and future prospects. Nat Rev Drug Discov 5(9):785–799. https://doi.org/10.1038/nrd2092
3. Armstrong PB, Quigley JP (1999) Alpha2-macroglobulin: an evolutionarily conserved arm of the innate immune system. Dev Comp Immunol 23(4–5):375–390
4. Barrett AJ, Starkey PM (1973) The interaction of alpha 2-macroglobulin with proteinases. Characteristics and specificity of the reaction, and a hypothesis concerning its molecular mechanism. Biochem J 133(4):709–724
5. Rehman AA, Ahsan H, Khan FH (2013) alpha-2-Macroglobulin: a physiological guardian. J Cell Physiol 228(8):1665–1675. https://doi.org/10.1002/jcp.24266
6. Marrero A, Duquerroy S, Trapani S, Goulas T, Guevara T, Andersen GR, Navaza J, Sottrup-Jensen L, Gomis-Ruth FX (2012) The crystal structure of human alpha2-macroglobulin reveals a unique molecular cage. Angew Chem Int Ed Engl 51(14):3340–3344. https://doi.org/10.1002/anie.201108015
7. Salvesen GS, Sayers CA, Barrett AJ (1981) Further characterization of the covalent linking reaction of alpha 2-macroglobulin. Biochem J 195(2):453–461
8. Nagasawa S, Han BH, Sugihara H, Suzuki T (1970) Studies on alpha 2-macroglobulin in bovine plasma. II. Interaction of alpha2-macroglobulin and trypsin. J Biochem 67(6):821–832
9. Herz J, Strickland DK (2001) LRP: a multifunctional scavenger and signaling receptor. J Clin Invest 108(6):779–784. https://doi.org/10.1172/JCI13992
10. Misra UK, Gonzalez-Gronow M, Gawdi G, Hart JP, Johnson CE, Pizzo SV (2002) The role of Grp 78 in alpha 2-macroglobulin-induced signal transduction. Evidence from RNA interference that the low density lipoprotein receptor-related protein is associated with, but not necessary for, GRP 78-mediated signal transduction. J Biol Chem 277(44):42082–42087. https://doi.org/10.1074/jbc.m206174200
11. Misra UK, Pizzo SV (2004) Potentiation of signal transduction mitogenesis and cellular proliferation upon binding of receptor-recognized forms of alpha2-macroglobulin to 1-LN prostate cancer cells. Cell Signal 16(4):487–496
12. Hoffman M, Pizzo SV, Weinberg JB (1988) Alpha 2 macroglobulin-proteinase complexes stimulate prostaglandin E2 synthesis by peritoneal macrophages. Agents Actions 25(3–4):360–367
13. Bonacci GR, Caceres LC, Sanchez MC, Chiabrando GA (2007) Activated alpha(2)-macroglobulin induces cell proliferation and mitogen-activated protein kinase activation by LRP-1 in the J774 macrophage-derived cell line. Arch Biochem Biophys 460(1):100–106. https://doi.org/10.1016/j.abb.2007.01.004
14. Anderson RB, Cianciolo GJ, Kennedy MN, Pizzo SV (2008) Alpha 2-macroglobulin binds CpG oligodeoxynucleotides and enhances their immunostimulatory properties by a receptor-dependent mechanism. J Leukoc Biol 83(2):381–392. https://doi.org/10.1189/jlb.0407236
15. Blacker D, Wilcox MA, Laird NM, Rodes L, Horvath SM, Go RC, Perry R, Watson B Jr, Bassett SS, McInnis MG, Albert MS, Hyman BT, Tanzi RE (1998) Alpha-2 macroglobulin is genetically associated with Alzheimer disease. Nat Genet 19(4):357–360. https://doi.org/10.1038/1243
16. Varma VR, Varma S, An Y, Hohman TJ, Seddighi S, Casanova R, Beri A, Dammer EB, Seyfried NT, Pletnikova O, Moghekar A, Wilson MR, Lah JJ, O'Brien RJ, Levey AI, Troncoso JC, Albert MS, Thambisetty M (2017) Alpha-2 macroglobulin in Alzheimer's disease: a marker of neuronal injury through the RCAN1 pathway. Mol Psychiatry 22(1):13–23. https://doi.org/10.1038/mp.2016.206
17. Werb Z, Burleigh MC, Barrett AJ, Starkey PM (1974) The interaction of alpha2-macroglobulin with proteinases. Binding and inhibition of mammalian collagenases and other metal proteinases. Biochem J 139(2):359–368
18. Caceres LC, Bonacci GR, Sanchez MC, Chiabrando GA (2010) Activated alpha(2) macroglobulin induces matrix metalloproteinase 9 expression by low-density lipoprotein receptor-related protein 1 through MAPK-ERK1/2 and NF-kappaB activation in

macrophage-derived cell lines. J Cell Biochem 111(3):607–617. https://doi.org/10.1002/jcb.22737
19. Tchetverikov I, Verzijl N, Huizinga TW, TeKoppele JM, Hanemaaijer R, DeGroot J (2003) Active MMPs captured by alpha 2 macroglobulin as a marker of disease activity in rheumatoid arthritis. Clin Exp Rheumatol 21(6):711–718
20. Arbelaez LF, Bergmann U, Tuuttila A, Shanbhag VP, Stigbrand T (1997) Interaction of matrix metalloproteinases-2 and -9 with pregnancy zone protein and alpha2-macroglobulin. Arch Biochem Biophys 347(1):62–68. https://doi.org/10.1006/abbi.1997.0309
21. Dufour A, Overall CM (2013) Missing the target: matrix metalloproteinase antitargets in inflammation and cancer. Trends Pharmacol Sci 34(4):233–242. https://doi.org/10.1016/j.tips.2013.02.004
22. Brkic M, Balusu S, Libert C, Vandenbroucke RE (2015) Friends or foes: matrix metalloproteinases and their multifaceted roles in neurodegenerative diseases. Mediators Inflamm 2015:620581. https://doi.org/10.1155/2015/620581
23. Jackson HW, Defamie V, Waterhouse P, Khokha R (2017) TIMPs: versatile extracellular regulators in cancer. Nat Rev Cancer 17(1):38–53. https://doi.org/10.1038/nrc.2016.115
24. Vandooren J, Van den Steen PE, Opdenakker G (2013) Biochemistry and molecular biology of gelatinase B or matrix metalloproteinase-9 (MMP-9): the next decade. Crit Rev Biochem Mol Biol 48(3):222–272. https://doi.org/10.3109/10409238.2013.770819
25. Vandooren J, Geurts N, Martens E, Van den Steen PE, Opdenakker G (2013) Zymography methods for visualizing hydrolytic enzymes. Nat Methods 10(3):211–220. https://doi.org/10.1038/nmeth.2371
26. Hannocks MJ, Zhang X, Gerwien H, Chashchina A, Burmeister M, Korpos E, Song J, Sorokin L (2017) The gelatinases, MMP-2 and MMP-9, as fine tuners of neuroinflammatory processes. Matrix Biol. https://doi.org/10.1016/j.matbio.2017.11.007
27. Vandooren J, Swinnen W, Ugarte-Berzal E, Boon L, Dorst D, Martens E, Opdenakker G (2017) Endotoxemia shifts neutrophils with TIMP-free gelatinase B/MMP-9 from bone marrow to the periphery and induces systematic upregulation of TIMP-1. Haematologica 102(10):1671–1682. https://doi.org/10.3324/haematol.2017.168799
28. Opdenakker G, Van den Steen PE, Dubois B, Nelissen I, Van Coillie E, Masure S, Proost P, Van Damme J (2001) Gelatinase B functions as regulator and effector in leukocyte biology. J Leukoc Biol 69(6):851–859
29. Van den Steen PE, Van Aelst I, Hvidberg V, Piccard H, Fiten P, Jacobsen C, Moestrup SK, Fry S, Royle L, Wormald MR, Wallis R, Rudd PM, Dwek RA, Opdenakker G (2006) The hemopexin and *O*-glycosylated domains tune gelatinase B/MMP-9 bioavailability via inhibition and binding to cargo receptors. J Biol Chem 281(27):18626–18637. https://doi.org/10.1074/jbc.M512308200
30. Rosenblum G, Van den Steen PE, Cohen SR, Grossmann JG, Frenkel J, Sertchook R, Slack N, Strange RW, Opdenakker G, Sagi I (2007) Insights into the structure and domain flexibility of full-length pro-matrix metalloproteinase-9/gelatinase B. Structure 15(10):1227–1236. https://doi.org/10.1016/j.str.2007.07.019
31. Overall CM, Butler GS (2007) Protease yoga: extreme flexibility of a matrix metalloproteinase. Structure 15(10):1159–1161. https://doi.org/10.1016/j.str.2007.10.001
32. Hu J, Yan M, Pu C, Wang J, Van den Steen PE, Opdenakker G, Xu H (2014) Chemically synthesized matrix metalloproteinase and angiogenesis-inhibiting peptides as anticancer agents. Anticancer Agents Med Chem 14(3):483–494
33. Van Leuven F, Cassiman JJ, Van den Berghe H (1981) Functional modifications of alpha 2-macroglobulin by primary amines. I. Characterization of alpha 2M after derivatization by methylamine and by factor XIII. J Biol Chem 256(17):9016–9022
34. Coan MH, Roberts RC (1989) A redetermination of the concentration of alpha 2-macroglobulin in human plasma. Biol Chem Hoppe Seyler 370(7):673–676
35. de Sain-van der Velden MG, Rabelink TJ, Reijngoud DJ, Gadellaa MM, Voorbij HA, Stellaard F, Kaysen GA (1998) Plasma alpha 2 macroglobulin is increased in nephrotic patients as a result of increased synthesis alone. Kidney Int 54(2):530–535. https://doi.org/10.1046/j.1523-1755.1998.00018.x
36. Vandooren J, Born B, Solomonov I, Zajac E, Saldova R, Senske M, Ugarte-Berzal E, Martens E, Van den Steen PE, Van Damme J, Garcia-Pardo A, Froeyen M, Deryugina EI, Quigley JP, Moestrup SK, Rudd PM, Sagi I, Opdenakker G (2015) Circular trimers of gelatinase B/matrix metalloproteinase-9 constitute a distinct population of functional enzyme molecules differentially regulated by tissue inhibitor of metalloproteinases-1. Biochem J 465(2):259–270. https://doi.org/10.1042/BJ20140418
37. Feldman SR, Rosenberg MR, Ney KA, Michalopoulos G, Pizzo SV (1985) Binding of alpha 2-macroglobulin to hepatocytes: mechanism of in vivo clearance. Biochem Biophys Res Commun 128(2):795–802
38. Mortensen SB, Sottrup-Jensen L, Hansen HF, Petersen TE, Magnusson S (1981) Primary and secondary cleavage sites in the bait region of alpha 2-macroglobulin. FEBS Lett 135(2):295–300
39. Gonias SL, Pizzo SV (1983) Reaction of human alpha 2-macroglobulin half-molecules with plasmin as a probe of protease binding site structure. Biochemistry 22(21):4933–4940
40. Dubois B, Starckx S, Pagenstecher A, Oord J, Arnold B, Opdenakker G (2002) Gelatinase B deficiency protects against endotoxin shock. Eur J Immunol 32(8):2163–2171. https://doi.org/10.1002/1521-4141(200208)32:8%3c2163:AID-IMMU2163%3e3.0.CO;2-Q
41. Vandooren J, Van Damme J, Opdenakker G (2014) On the structure and functions of gelatinase B/matrix metalloproteinase-9 in neuroinflammation. Prog Brain Res 214:193–206. https://doi.org/10.1016/B978-0-444-63486-3.00009-8
42. Gao M, Nguyen TT, Suckow MA, Wolter WR, Gooyit M, Mobashery S, Chang M (2015) Acceleration of diabetic wound healing using a novel protease-anti-protease combination therapy. Proc Natl Acad Sci USA 112(49):15226–15231. https://doi.org/10.1073/pnas.1517847112
43. Opdenakker G, Van Damme J, Vranckx JJ (2018) Immunomodulation as rescue for chronic atonic skin wounds. Trends Immunol 39(4):341–354. https://doi.org/10.1016/j.it.2018.01.010
44. Nagase H, Itoh Y, Binner S (1994) Interaction of alpha 2-macroglobulin with matrix metalloproteinases and its use for identification of their active forms. Ann N Y Acad Sci 732:294–302
45. Wang M, Zhang Q, Zhao X, Dong G, Li C (2014) Diagnostic and prognostic value of neutrophil gelatinase-associated lipocalin, matrix metalloproteinase-9, and tissue inhibitor of matrix metalloproteinases-1 for sepsis in the Emergency Department: an observational study. Crit Care 18(6):634. https://doi.org/10.1186/s13054-014-0634-6
46. Wang L, Wei C, Deng L, Wang Z, Song M, Xiong Y, Liu M (2018) The accuracy of serum matrix metalloproteinase-9 for predicting hemorrhagic transformation after acute ischemic stroke: a systematic review and meta-analysis. J Stroke Cerebrovasc Dis 27(6):1653–1665. https://doi.org/10.1016/j.jstrokecerebrovasdis.2018.01.023
47. Marchesi C, Dentali F, Nicolini E, Maresca AM, Tayebjee MH, Franz M, Guasti L, Venco A, Schiffrin EL, Lip GY, Grandi AM (2012) Plasma levels of matrix metalloproteinases and their inhibitors in hypertension: a systematic review and meta-analysis. J Hypertens 30(1):3–16. https://doi.org/10.1097/HJH.0b013e32834d249a
48. Zhong C, Yang J, Xu T, Xu T, Peng Y, Wang A, Wang J, Peng H, Li Q, Ju Z, Geng D, Zhang Y, He J, Investigators C (2017) Serum

matrix metalloproteinase-9 levels and prognosis of acute ischemic stroke. Neurology 89(8):805–812. https://doi.org/10.1212/WNL.0000000000004257

49. Prince HE (2005) Biomarkers for diagnosing and monitoring autoimmune diseases. Biomarkers 10(Suppl 1):S44–S49. https://doi.org/10.1080/13547500500214194
50. Gimeno-Garcia AZ, Trinanes J, Quintero E, Salido E, Nicolas-Perez D, Adrian-de-Ganzo Z, Alarcon-Fernandez O, Abrante B, Romero R, Carrillo M, Ramos L, Alonso I, Ortega J, Jimenez A (2016) Plasma matrix metalloproteinase 9 as an early surrogate biomarker of advanced colorectal neoplasia. Gastroenterol Hepatol 39(7):433–441. https://doi.org/10.1016/j.gastrohep.2015.10.002
51. Vandooren J, Geurts N, Martens E, Van den Steen PE, Jonghe SD, Herdewijn P, Opdenakker G (2011) Gelatin degradation assay reveals MMP-9 inhibitors and function of *O*-glycosylated domain. World J Biol Chem 2(1):14–24. https://doi.org/10.4331/wjbc.v2.i1.14
52. Paemen L, Martens E, Masure S, Opdenakker G (1995) Monoclonal antibodies specific for natural human neutrophil gelatinase B used for affinity purification, quantitation by two-site ELISA and inhibition of enzymatic activity. Eur J Biochem 234(3):759–765